Atmospheric Environment 50 (2012) 120–128

Contents lists available at SciVerse ScienceDirect

Atmospheric Environment

journal homepage: www.elsevier.com/locate/atmosenv

Exploration of effects of a vegetation barrier on particle size distributions in a near-road environment

Jonathan T. Steffens, Yan Jason Wang, K. Max Zhang*

Sibley School of Mechanical and Aerospace Engineering, Cornell University, Ithaca, NY 14853, USA

ARTICLE INFO

Article history:
Received 7 November 2011
Received in revised form
20 December 2011
Accepted 21 December 2011

Keywords:
Air quality
Aerosol
Vegetation
Dry deposition
Ecosystem services

ABSTRACT

Roadside vegetation barriers have been suggested as a potential mitigation strategy for near-road air pollution. However, there is still a lack of mechanistic understanding of how roadside barriers affect pollutant transport and transformation on and near roadways, especially under different meteorological conditions and barrier properties. In this study, we incorporated the representations of particle aerodynamics and deposition mechanisms into the Comprehensive Turbulent Aerosol Dynamics and Gas Chemistry (CTAG) model, and explored the effects of vegetation barriers on near-road particulate air pollution by comparing the simulation results against field measurements. The model shows generally adequate agreement with concentrations of particles larger than 50 nm but tends to overpredict concentrations of particles less than 50 nm behind a vegetation barrier. Sensitivity tests were performed by comparing two different particle dry deposition models and varying the vegetation density and local meteorology. It was found that an increase in leaf area density (LAD) further reduces particle concentration, but the responses were non-linear. Increases in wind speed were shown to enhance particle impaction, but reduce particle diffusion, which result in reduction in concentration for particles larger than 50 nm but have a minimal effect on particles smaller than 50 nm. Further improvements in representing particle deposition and aerodynamics in near-road environments are needed to fully capture the complex effects of roadside vegetation barriers.

© 2011 Elsevier Ltd. All rights reserved.

1. Introduction

Exposure to traffic-related air pollutants has been linked to a wide variety of health concerns, including respiratory and cardiovascular problems, birth and developmental defects, and cancer (HEI, 2010). Given the enormous health and societal impacts resulting from near-road air pollution, it is critical to develop effective strategies to mitigate near-road air pollution. In addition to vehicle emissions control, there are potential opportunities for mitigating near-road air pollution in roadway design options that affect pollutant transport and dispersion such as road configurations and the presence of roadside barriers (Bowker et al., 2007; Baldauf et al., 2008; Cahill, 2010). Recent wind tunnel and field studies (Heist et al., 2009; Finn et al., 2010) have suggested that roadside barriers, such as sound walls and vegetation, may provide a cost effective strategy to mitigate near-road air pollution. However, there is still a lack of mechanistic understanding of how roadside barriers affect pollutant transport and transformation on and near roadways, especially under different meteorological conditions and barrier properties.

In this paper, we attempt to explore the effects of roadside vegetation barriers on transport of exhaust particles near roadways. The presence of vegetation barriers affects two major atmospheric processes governing the plume transport near roadways, i.e., turbulent mixing and dry deposition of atmospheric constituents. These two processes have been studied by separate communities. First, windbreak/shelterbelt and meteorological research communities have long focused on the aerodynamic aspects of vegetation barriers, i.e., how porous heterogeneous vegetative structures affect the wind field, microclimate and boundary layer meteorology (Cleugh, 1998; Wilson, 2004a, 2004b; Santiago et al., 2007). Second, the deposition of gaseous and particulate species on vegetation canopies has been an active research area in aerosol science, and several deposition models have been proposed and implemented in multi-scale air quality and ecological models. There are only few modeling studies so far which have investigated how the vegetation affects plume transport. However, they did not consider pollutant deposition (Raupach et al., 2001; Bouvet et al., 2007; Gromke and Ruck, 2007; Gromke et al., 2008; Buccolieri et al., 2009).

* Corresponding author. Cornell University, Sibley School of Mechanical and Aerospace Engineering, 287 Grumman Halll thaca, NY 14853, USA.
E-mail address: kz33@cornell.edu (K.M. Zhang).

1352-2310/$ – see front matter © 2011 Elsevier Ltd. All rights reserved.
doi:10.1016/j.atmosenv.2011.12.051

In this paper, we expand the capability of the Comprehensive Turbulent Aerosol Dynamics and Gas Chemistry (CTAG) model to characterize the aerodynamic and deposition effects of roadside vegetation barriers. The focus of this paper will be to evaluate the model performance against experimental results from a recent field measurement conducted in Chapel Hill, NC. This study marks the first time the effects of aerodynamics, particle deposition and plume transport have been combined into a single model, constrained by experimental data. While aerodynamic vegetation models have been developed for use in local environments, vegetation deposition models are typically developed for larger forest canopies and for use in large-scale regional models. While not conclusive, the simulation results will give insight into the performance of the deposition models of Zhang et al. (2001) and Petroff and Zhang (2010) at the local level. In addition, sensitivity analyses will be performed to predict how the near-road air quality will respond to changes in parameters such as modeling geometry, upwind meteorological conditions and canopy leaf area density.

2. Model description

CTAG is an environmental turbulent reacting flow model, designed to simulate transport and transformation of multiple air pollutants in complex environments, e.g., from emission sources to ambient background. CTAG has been applied to a wide variety of urban environments ranging from on-road modeling to simulation of several square kilometers (Wang and Zhang, 2009, submitted for publication; Wang et al., 2011; Wang et al., submitted for publication; Tong et al., 2012). Next, we will describe how we implement the effects of vegetation barriers based on the CTAG framework.

2.1. Eulerian–Lagrangian framework

We adopt an Eulerian framework in order to simulate the flow field, and utilize a Lagrangian framework to simulate the motion of particles within the flow field. The aerosol dynamics model consists of several components: advective transport, deposition, and coagulation. Additional aerosol processes, such as evaporation and condensation, were not modeled in this study. It is assumed that the residence time in the domain, which is estimated to be less than 10 s for the modeling scenarios presented in the paper, is too short for these processes to have any significant impact on the results (Zhang and Wexler, 2004; Zhang et al., 2004)

Advective transport is processed by the Discrete Phase Model (DPM), which computes a force balance on a representative number of fluid particles and tracking them as they move through the domain (ANSYS Inc. 2009). Each tracked particle actually represents a large number of physical particles. The ratio of tracked particles to physical particles is referred to as the particle strength. The particle size distributions are divided into discrete size bins. In this study, we chose 9 size bins, evenly spaced in the logarithm scale. Within the Lagrangian framework, each tracked particle is assumed to be a self-contained representation of the entire particle distribution. That is, each tracked particle will have its own size distribution profile which updates at each time step of the simulation.

After the particles have been tracked throughout the entire simulation domain, local concentrations are calculated by averaging the concentrations of the tracked particles that pass through a given area (ANSYS Inc. 2009).

2.2. Aerodynamic model

We employ ANSYS Fluent commercial software package (ANSYS Inc. 2009) as the turbulence solver. The flow field is resolved by iteratively solving the mass conservation equation and the Reynolds Averaged Navier–Stokes (RANS) equations. The turbulence field is computed using a realizable k-ε model (Jones and Launder, 1972), which uses two equations to solve the turbulent kinetic energy, k, and the turbulent dissipation rate, ε.

2.2.1. Spatial averaging

Vegetation consists of numerous small leaf and branch structures that cause drag which impedes the motion of incoming wind, which in turn significantly influences the turbulence characteristics of the flow. This highly complex structure found within plant canopies makes it impossible to completely resolve every physical element in a computational model due to the prohibitively large computation power this would require. In order to overcome this challenge, the vegetation is spatially averaged in order to produce average wind speed and turbulence statistics within the canopy (Wilson and Shaw, 1977; Wang et al., 2001). The canopy, which in reality exists as both fluid and solid material, is represented by a region of fluid only. The solid components of the canopy are not physically modeled. The effects of the solid matter manifest as source and sink terms to the prognostic equations. By using this method, the effects of the solid elements of the canopy can be modeled without having to physically resolve them. If the model is perfectly accurate, the velocity and turbulence statistics of each cell in the simulation will be the average over that same volume in the physical system. Recently, Endelew et al. (2009) proposed a hybrid model that represents the trunk and largest branches as solid and only spatially averages the smaller branches and leaf elements. However, the hybrid method requires explicit knowledge of canopy geometry such as trunk size and branch number and location, which is unavailable for this study.

2.2.2. Windbreak effects

The vegetation imposes a drag on the air moving through the leaves and branches. This flow obstruction causes some air to move up and around the canopy, thus increasing vertical mixing (Cahill, 2010). In addition, this drag creates a windbreak effect behind the barrier which is characterized by lower wind speed and lower turbulence in the wake of the canopy (Wang et al., 2001; Cleugh, 1998; Santiago et al., 2007; Wilson, 2004a, 2004b). Since the windbreak effect decreases wind speed downwind of the barrier, it decreases the rate at which traffic-related pollutants can be advectively transported away, which can potentially increase the pollutant concentrations.

The momentum drag due to vegetation is proportional to the plant coefficient of drag, C_d (dependent on the tree type) and the leaf area density, LAD (ratio of leaf surface area to total volume occupied by vegetative element). Thom (1972) gives the modeled sink term, S_u, to be:

$$S_u = -\rho C_D \mathrm{LAD} u^2 \quad (1)$$

As air moves through the canopy, small leaf and stem elements disturb the mean flow and convert kinetic energy to turbulent kinetic energy. However, this turbulence is rapidly dissipated. Thus, within the canopy, turbulence may be high but there is a low turbulence regime behind the canopy (Kaimal and Finnigan, 1994). Thus, TKE is modeled as a combination of a source term representing the creation of TKE, and a sink term relating to the rapid dissipation of eddies.

The model formulation used to describe the windbreak effect is dependent on the turbulence solver being employed. For example, if using the k-ε turbulence solver, source and sink terms must be added to both the turbulent kinetic energy equation and the turbulent dissipation equation. There has been significant research

into this closure problem for turbulence in plant canopies and several models have been developed (Green et al., 1995; Hiraoka and Ohashi, 2008). The second order k-ε- model created by Green (1992) is used in this paper and is given by:

$$S_k = \rho C_D \mathrm{LAD}\left(\beta_p u^3 - \beta_d u k\right) \quad (2)$$

where β_p is the fraction of mean flow converted to turbulent kinetic energy and β_d is fraction of turbulent kinetic energy dissipated within the canopy (Green, 1992). Liu et al. (1996) used dimensional analysis to create a model for the dissipation rate source term which shows good agreement with wind tunnel data, given by:

$$S_\varepsilon = \rho C_D \mathrm{LAD}\left(C_{\varepsilon 4}\beta_p \frac{\varepsilon}{k} u^3 - C_{\varepsilon 5}\beta_d u \varepsilon\right) \quad (3)$$

$$\beta_d = C_\mu^{1/2}\frac{2^{2/3}}{\alpha}\beta_p + \frac{3}{\sigma_k} \quad (4)$$

$$\alpha = \frac{1}{2C_D \mathrm{LAD} C_\mu^{3/4} k^{3/2}/\varepsilon} \quad (5)$$

where $\beta_p = 1$ if one assumes a dense canopy (Walklate et al., 1996), and $C_{\varepsilon 4}$, $C_{\varepsilon 5}$, C_μ and σ_k are constants defined in the k-ε model.

2.3. Lagrangian Aerosol Dynamics model

2.3.1. Particle aerodynamics

Particle transport is determined by the drag force enacted on the particle from the bulk flow in addition to gravitational settling. Normally, Brownian motion is considered for sub-micrometer particles. However, for turbulent flows, turbulent diffusion, due to random particle movement caused by turbulent eddies is much greater than that from Brownian motion. Therefore all random motion is modeled as a Discrete Random Walk Model (ANSYS Inc. 2009) which works by adding a random velocity perturbation to the average velocity.

2.3.2. Dry deposition

It is assumed that when a particle is intercepted by a solid surface, it is deposited and removed from the airflow. However, due to the spatial averaging described in Section 2.2.1, which removes physical surfaces from the modeled canopy, a statistical dry deposition model must be used. A number of dry deposition models of atmospheric particles have been proposed and implemented in multi-scale air quality and ecological models by calculating a deposition velocity, v_d (Davidson et al., 1982; Slinn, 1982; Shimeta and Jumars, 1991; Zhang et al., 2001, 2009; Piskunov, 2009, Petroff et al., 2009; Petroff and Zhang, 2010).In our study, we have implemented the dry deposition models proposed by Zhang et al. (2001) and Petroff and Zhang (2010), which show good agreement with field measurements.

The actual change in the particle concentration, C, is dependent not only on the deposition velocity but also on the density of the vegetation and the concentration itself. The following equation is used to compute deposition rate:

$$\frac{\partial C}{\partial t} = -\mathrm{LAD} v_d C \quad (6)$$

Equation (6) applies to both particle number and mass concentrations. As we model particle size distributions as discrete size bins, Equation (6) is used to update the particle strength for each bin by assuming the percent change in tracked particle strength is equal to the percent change in particle concentration.

2.3.3. Coagulation

Coagulation occurs when two distinct particles collide to form a single, larger particle. We adopt a semi-implicit modeling scheme to simulate coagulation described by Jacobson (2005).

3. Measurement data

The detailed description of the field measurements to characterize the effects of solid and vegetative barriers on near-road air quality in North Carolina was provided by Hagler et al. (in press). A brief summary is presented here. Stationary air quality monitoring was performed at vertical heights of 3 m and 7 m behind the barrier and 3 m away from the barrier. The coordinates of the measurement sites behind the barrier and away from the barrier are 35.914469,−79.026081 and 35.911403,−79.026217 respectively. The vegetative barrier consisted of a mix of pine and cedar tree. Wind speed and direction measurements were collected using a 3-D ultrasonic anemometer with sampling frequency 1 Hz. Ultrafine particle (UFP) size distributions were obtained using a scanning mobility particle sizer (SMPS), which captured 88 size channels ranging from 12.6 to 289 nm with a sampling frequency of 120 s. In addition, a mobile sampling vehicle measured UFPs while driving on a route, including background areas far from the roadway, using a fast mobility particle sizer (FMPS). Refer to Hagler et al. (in press) for detailed instrumentation information. In addition to performing the field sampling at different roadside locations, instrument intercomparison was frequently performed by co-locating the particle instruments for approximately 30 min of time. The measurements shown in this paper were from a single morning sampling session in Chapel Hill, NC along U.S. Route 15–501 on November 23, 2008. The site can be seen from satellite view obtained from a Google Maps image in Fig. 1. This site had an approximately 6–8 m tall evergreen tree stand (conifers) located

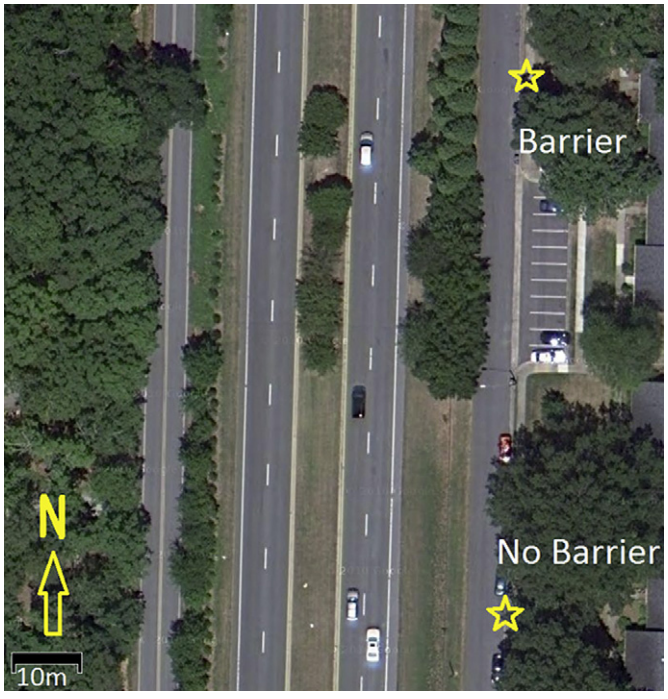

Fig. 1. Plan view of the sampling locations (marked by stars) near NC Highway 15–501 in Chapel Hill.

adjacent to the route for a stretch of the roadway. To correct for any instrument biases and allow the multiple data sets to be compared, data from co-located sampling of three SMPS units and the one FMPS unit were used to develop correction factors, based on assigning one of the SMPS units as a reference.

4. Modeling scenarios

Since this study represents the first atmospheric modeling effort of pollutant transport through roadside vegetation barriers, the model formulation will only take into account a steady-state meteorological inlet condition, using average values for velocity and wind direction. The steadiness of the meteorology was evaluated on two conditions: velocity magnitude and wind direction. A 5 min moving average of wind speed was plotted as shown in Fig. 2. By visual inspection, it is obvious that the wind speed is more constant earlier in the day, from about 7:00 to 7:45. The wind speeds measured over this period are low, with an average of 0.57 m s^{-1}. Using the method of Yamartino (1984), the calmest time period was found to be from 7:00 AM to 7:45 AM, with a wind standard deviation of 48°. Therefore, we will focus on this time period for the study. It is notable that 48° represents a large standard deviation. Sensitivity analysis was performed by varying the wind direction plus or minus one standard deviation. It was found that at the most extreme case the particle size distribution results varied at most 15%. We further separate this period into three modeling scenarios, namely Morning, Peak 1, and Peak 2. Peak 1 and Peak 2 represent two spikes in particle number concentrations that occurred 1) when there were no drastic changes in wind velocity and wind speed, and 2) at both the no-barrier site and 3 m height behind the barrier. These time periods can be seen in Fig. 3. Therefore, Peak 1 and Peak 2 captured two single plumes from traffic under steady meteorological conditions. The remaining times, when the particle number concentrations are relatively steady, are averaged and are referred to as the Morning modeling scenario throughout the paper.

5. Geometry, boundary conditions and emissions

The computational domain was created using overhead satellite imagery to map the sampling area. Canopy heights were measured on site during the field study. Fig. 4 shows the schematic of the finalized geometry. The major elements of the domain are the tree stand, the upwind and downwind canopies and a highway

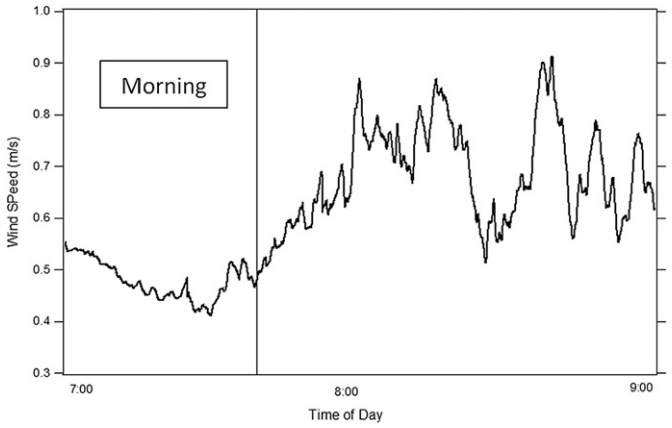

Fig. 2. Wind speed 5 min moving average with Morning modeling scenario represented.

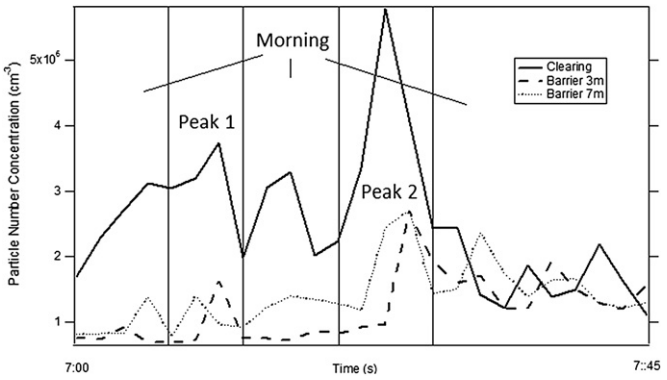

Fig. 3. Particle number concentration for barrier and no-barrier. Three modeling scenarios (Morning, Peak 1, and Peak 2) represented.

emissions zone. The domain has dimensions of 400 m long by 400 m wide by 100 m high, divided into 4.1 million elements.

A small highway emission zone is created. This region is used to provide a source of particle emissions as well as vehicle-induced turbulence (VIT). The height of this zone is taken to be roughly the height of the vehicular traffic moving along the highway (Wang and Zhang, 2009). Since the traffic on the studied highway is dominated by passenger vehicles, the height of the emissions zone is chosen to be 2 m (Wang et al., 2011). The size distribution profile of particle emissions released from this zone is set such that the particle size distribution simulated at the no-barrier site matches that of the experiment. The emissions released from the highway zone were taken to be constant. As vehicles travel along the roadway, they perturb the airflow, increasing the turbulence in the airflow. VIT is generated using the parameterization developed by Wang and Zhang (2009) and Wang et al. (2011).

Upwind of the highway is a forest canopy of evergreen species, which is included in the model in order to allow the flow over the highway to develop naturally. The tree stand is positioned downwind of the highway, as well as the canopy further downwind of the measurement site. The small row of trees in the middle of the highway, seen in Fig. 1, was not represented due to their small size (roughly 3 m in height) and low density.

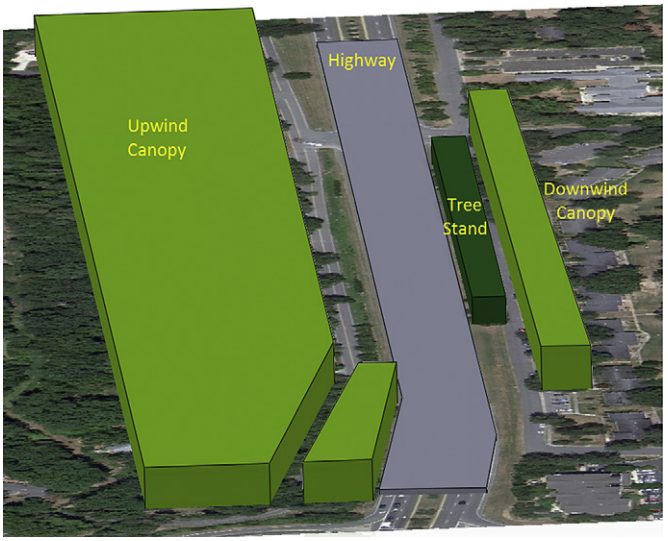

Fig. 4. Computational domain showing highway, tree stand, upwind and downwind canopy.

It is important to accurately represent the vegetation's LAD, which is a function of height. The leaf area index (LAI) is a closely related parameter which measures the ratio of leaf surface area to ground surface are. It was measured for the site and found to be 3.3 +/− 1.0 (Hagler et al., in press). The relationship between LAI and LAD is defined as:

$$\mathrm{LAI} = \int_0^h \mathrm{LAD}\,dz \tag{7}$$

While the LAI is not sufficient to determine the vertical profile of LAD, it does offer an important constraint. Lalic and Mihailovic (2004) offer an empirical relationship to describe LAD as a function of height given by:

$$\mathrm{LAD} = L_m\left(\frac{h-z_m}{h-Z}\right)^n \exp\left[n\left(1-\frac{h-z_m}{h-Z}\right)\right],$$
$$n = \begin{cases} 6, & 0 \le z < z_m \\ 1/2, & z_m \le z \le h \end{cases} \tag{8}$$

where h is the canopy height, L_m is the maximum LAD and z_m is the location at which maximum LAD occurs. Lalic and Mihailovic (2004) recommend that for conifers $z_m = 0.4\,h$. The only remaining parameter, L_m, can be obtained by numerically integrating Equation (7). The LAD profile obtained from this method is shown in Fig. 5.

In addition to the geometry, boundary conditions are required in order to perform simulation. The ground is defined as a no slip wall. The western side of the domain is defined as a velocity inlet condition, where profiles of velocity and TKE must be provided. The eastern side is set to be an outlet condition. The northern and southern sides are defined as periodic conditions. This essentially allows for inlet airflow to be at any arbitrary angle and still be uniform as it exits the inlet forest canopy. The top of the domain, assumed to be high enough to not affect ground level wind flow, imposes no shearing force and is thus given a condition of no velocity gradient.

Inlet conditions are important for flow simulations and the results are sensitive to those chosen. Fig. 1 shows that upwind of the highway, there is a fairly uniformly forested area. Cowan (1968) has created an equation to characterize the velocity profile through a forest canopy given by:

$$u = u_h\left[\frac{\sin\beta\frac{z}{h}}{\sin\beta}\right]^{\frac{1}{2}} \tag{9}$$

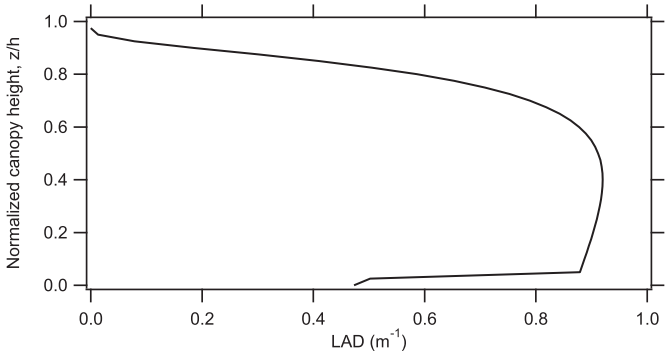

Fig. 5. The derived LAD profile of the model vegetation barrier from observed LAI.

where u_h is the wind velocity at the top of the canopy and h is the canopy height. β is defined as the extinction factor and is given by (Massman, 1987):

$$\beta = \frac{4C_D\mathrm{LAD}}{\alpha^2\kappa^1} \tag{10}$$

where κ is the von Karman constant and is typically given to be 0.4 and z_0 is the canopy roughness height and α describes the vegetative roughness and varies between 1 and 2 (Raupach and Thom, 1981). Above the canopy, the classical logarithmic atmospheric boundary layer profile is used given by:

$$\frac{u}{u_*} = \frac{1}{k}\ln\left(\frac{z-d}{z_0}\right) \tag{11}$$

The friction velocity, u_*, is not known exactly for the modeling scenario. However, it has been estimated by matching this profile to the one given in Equation (9) at the top of the canopy. However, the velocity and turbulence characteristics are known at the no-barrier site on the other end of the highway. The velocity profile will evolve as it travels along the domain, but it is possible to vary the parameters of the inlet profile until the wind field in the simulation matches that of the measured data at the no-barrier site. In this manner, some of the uncertainty is removed from the inlet boundary condition. Additionally, a sensitivity test is performed by varying the inlet parameters to gauge how the importance of the inlet parameters on concentrations.

6. Results and discussions

Simulation results were obtained for the morning time period as well as the two separate peak periods. Additionally, we performed simulations to test the sensitivity of the model to geometry, upwind meteorology and vegetation leaf area.

6.1. Velocities

Table 1 shows the comparison of velocity behind the barrier between simulation and experiment for the morning period as well as each of the peak times. The velocity at a height of 3 m captures the general trend of reduced wind speed behind the barrier. However, the model is unable to accurately capture the velocity at the 7 m height. Since there is no corresponding 7 m velocity measurement at the no-barrier site, it is impossible to know what the vertical profile of velocity actually looks like. It is possible that the profiles obtained from literature do not accurately reflect the local meteorology. It is also possible that since the measurement point in near the top of the barrier, and that the barrier height is not perfectly uniform as it was modeled, that the errors lie in the geometric construction of the model. The Morning and Peak 1 modeling scenarios show the velocity to be lower at 7 m than at 3 m. Various inlet velocity profiles were simulated, and none were able to match this trend in the data. A sensitivity analysis will be

Table 1
Wind speed experimental data and simulation results.

Period	Experimental velocity (m s^{-1})			Simulation velocity (m s^{-1})	
	No-barrier 3 m	Barrier 3 m	Barrier 7 m	Barrier 3 m	Barrier 7 m
Morning	0.57	0.22	0.03	0.23	0.30
Peak 1	0.61	0.15	0.12	0.25	0.40
Peak 2	0.32	0.09	0.22	0.18	0.22

performed to investigate how the flow field will affect particle size distributions discussed in Section 6.3.5.

6.2. Size distributions

Fig. 6 illustrates the comparisons between measured and predicted particle size distributions behind the barriers at the heights of 3 m and 7 m for the three simulated periods (i.e., the morning period and two peak periods) for both the Zhang et al. (2001) and the Petroff and Zhang (2010) deposition models. As described earlier, the size distributions at the no-barrier site match the measured values by adjusting the emission profiles.

Regardless of the dry deposition model, all of the simulations predict that more reduction in particle concentration occurs at 3 m than at 7 m, which agrees with the trend observed in the experimental data. The model predictions using the Zhang et al. (2001) dry deposition model show closer agreement with the measured values than those using the Petroff and Zhang (2010) dry deposition model, particularly for particle sizes below 100 nm. It should be noted that despite the discrepancies observed in the velocity measurements, the size distribution simulations perform reasonably well. There are several possible reasons to explain this phenomenon. First, since most of the dilution takes place before the barrier, and the velocity conditions in the simulation were such that they matched the experimental data, dilution should not be significantly different. Second, deposition only occurs within the canopy. However, the wind speed measurements taken in the experiment are several meters behind the barrier. It is possible that other factors, such as vegetation or other obstacles further downwind of the measurement point affected the velocity measurements but did not alter wind flow through the canopy.

For the two peak periods, the model captures the experimental concentrations with varying degrees of success. As seen with the morning period case, the model tends to predict concentrations higher than observed in the experiment in the less than 50 nm size range. The concentration differs significantly between the predicted and measured values for the first peak period in the smaller size ranges, while the comparison is quite good during the second

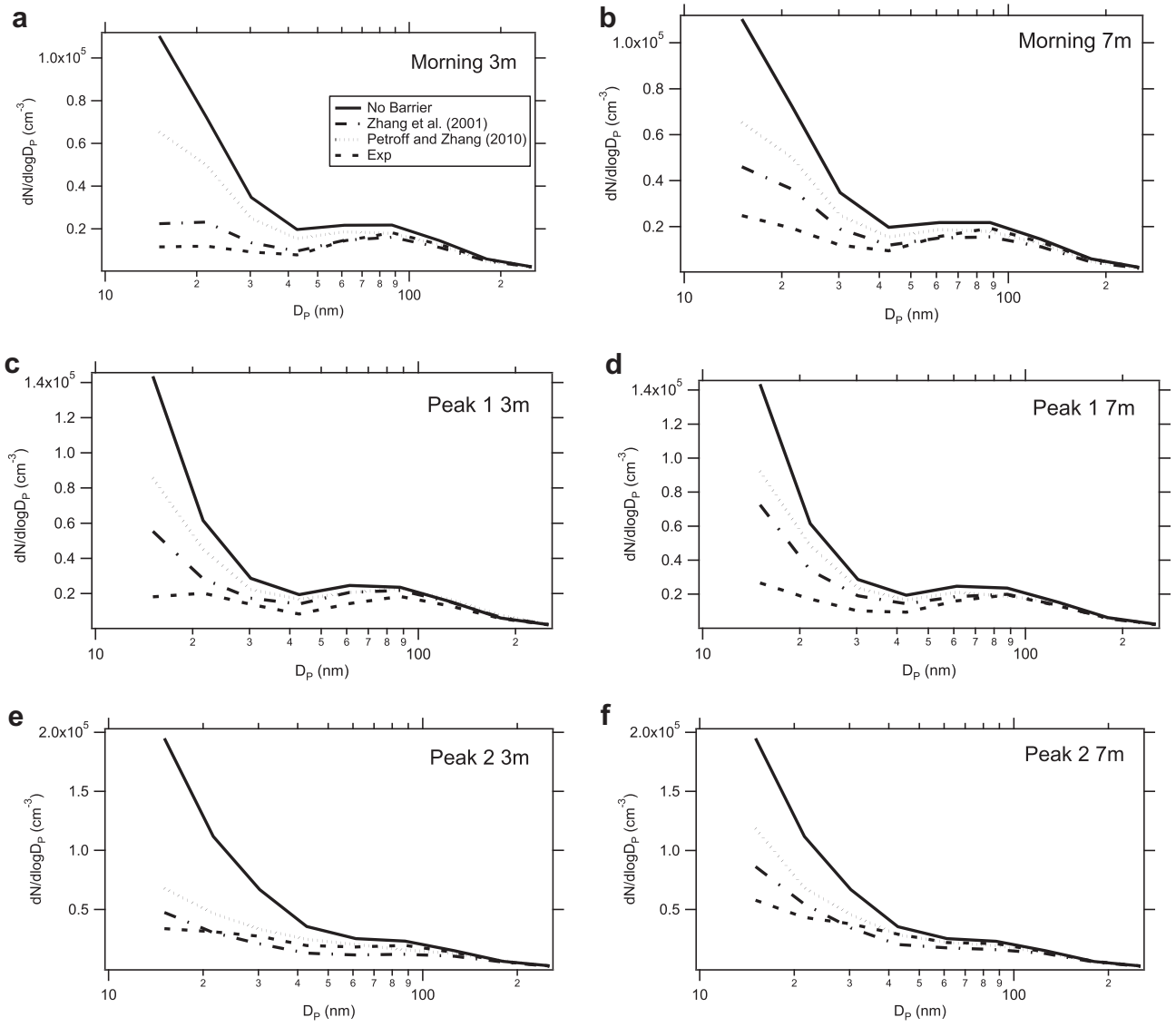

Fig. 6. Size distribution profile comparing simulation to experiment at 3 m and 7 m height for modeling scenario a) Morning 3 m, b) Morning 7 m, c) Peak 1 3 m, d) Peak 1 7 m, e) Peak 2 3 m, f) Peak 2 7 m. Non-Solid lines represent concentration behind the barrier. Solid line representing no-barrier site provided to illustrate concentration reduction due to the barrier.

peak period. It should be noted that the second peak period also showed the best agreement with the velocity measurement, while the morning and first peak period had larger discrepancies. It is likely that the errors in the flow model have a larger impact on particles less than 50 nm in diameter and that improvements to the flow field model may have a significant improvement in the particle concentration model. Further analyses on the effects of flow fields are described in Section 6.3.5.

6.3. Sensitivity analyses

Various sensitivity studies were performed to examine how varying the model parameters affects the simulation results. For these sensitivity tests, the morning period was used as a baseline case.

6.3.1. Deposition velocities

Fig. 7 shows the deposition velocity profiles for the morning case obtained from the two dry deposition models compared with the deposition velocity profile required to produce the reduction in concentration observed during the morning period. As expected from Fig. 6, the Zhang et al. (2001) model shows better agreement for particles less than 50 nm in diameter and the results overall. It should be noted, however, that both models were developed and validated with forest canopy field data, and not that of isolated tree stands. This may be a contributing factor for the observed discrepancies.

6.3.2. Coagulation

Simulations were performed both with and without the coagulation model. The difference in particle residence time behind the barrier and away from the barrier was approximately 1 to 5 s depending on the parameters. However, such a short time was unable to produce any distinction between the simulation with and without the effects of coagulation taken into consideration.

6.3.3. Presence of surrounding vegetation

One possible concern is how the presence of the vegetation downwind of the measurement site affects those measurements. For this sensitivity test, the downwind vegetation was removed. It was found that doing so had negligible effect on the measured velocity at 3 m and increased the velocity at 7 m from 0.30 m s^{-1} to 0.35 m s^{-1}. However, wind speed within the canopy differed by at most 1 percent. Additionally, we simulated the case where the downwind vegetation was doubled in leaf density. We found again, that this had a negligible effect on the concentration profile.

6.3.4. Leaf area density (LAD)

LAD is a key parameter determining the amount of deposition that takes place within the canopy (Petroff et al., 2009). For the dependency on leaf area, three additional cases were run by multiplying the baseline leaf area density profile by a constant value to account for the effects on wind speed and deposition. Changes in vertical LAD profile may also have an effect on vertical concentration but were not considered in this study, since we only compare simulation to experiment at one height.

The three cases used leaf areas of 50, 150, and 250 percent of the baseline leaf area. Fig. 8 shows concentration ratio between the barrier and the no-barrier site, C_B/C_C, at a height of 3 m. Higher LAD leads to more deposition. The 150% LAD case agrees very well with the experimental data in the less than 50 nm size range. However, it overpredicts concentration reduction in the larger size ranges by up to 50%. This suggests that variation of leaf area alone is insufficient in accounting for the differences between the model and the field data. It should be noted that the change in C_B/C_C is not linearly proportional to the change in LAD and affects different size ranges differently. For instance, at 50% LAD, compared to the baseline LAD, C_B/C_C is 2.2 times greater for 15 nm particles but only 1.2 times greater for the 273 nm particles. Conversely, at 250% LAD, compared to the baseline LAD, C_B/C_C is 7.4 times smaller for the 15 nm particles and only 1.2 times smaller for the 273 nm particles.

6.3.5. Wind speed

It is also a possibility that the differences between the model and the experiment are due to uncertainties in the local meteorology. Similar to the LAD sensitivity test, the inlet meteorology sensitivity study was performed by multiplying the inlet velocity profile by a constant value. The cases performed were for inlet velocities of 50, 150 and 250 percent the baseline velocity. C_B/C_C for each velocity is shown in Fig. 9. For the size ranges below 50 nm, the reductions in concentration are similar for all wind speeds except the 50% velocity, which is significantly higher. There is a larger difference observed in particles greater than 50 nm in diameter. There are several competing processes which influence these changes in C_B/C_C. First, as wind speed increases, the aerodynamic resistance term in the deposition model decreases, thus increasing deposition caused by impaction. Second, an increase in wind speed decreases the residence time of the particle within the canopy. This allows less time for diffusion, thus decreasing deposition. However, this does not influence impaction, since that process is not governed by how long the particle resides in the canopy but rather how likely it is to contact a solid surface as it moves through it. Third, at higher wind speeds, the particles experience more efficient vertical mixing, further enhancing the

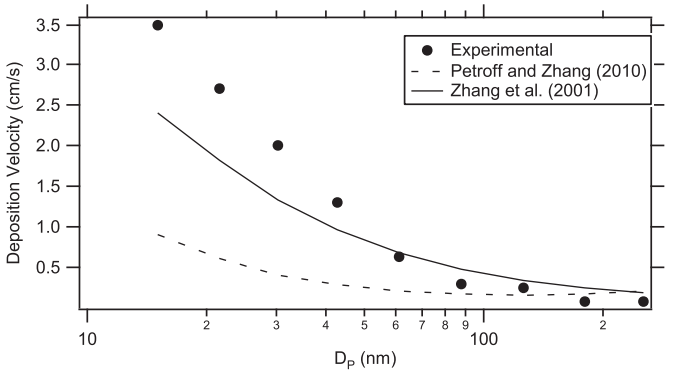

Fig. 7. Deposition velocity curves for morning period for Petroff and Zhang (2010) and Zhang et al. (2001) models as well as deposition velocities required to exactly match experimental results.

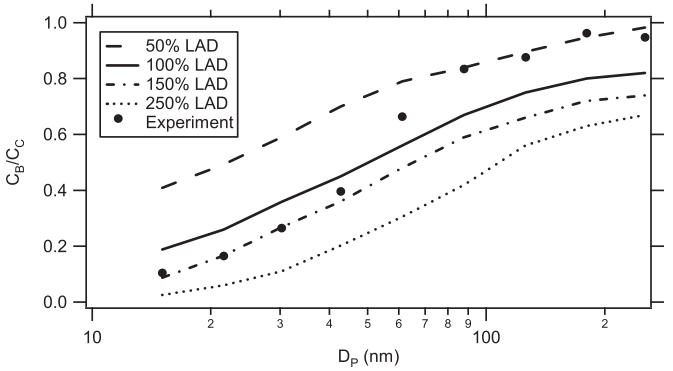

Fig. 8. Comparison of concentration ratio between the barrier and the no-barrier sites, C_B/C_C, for varying multiples of baseline LAD.

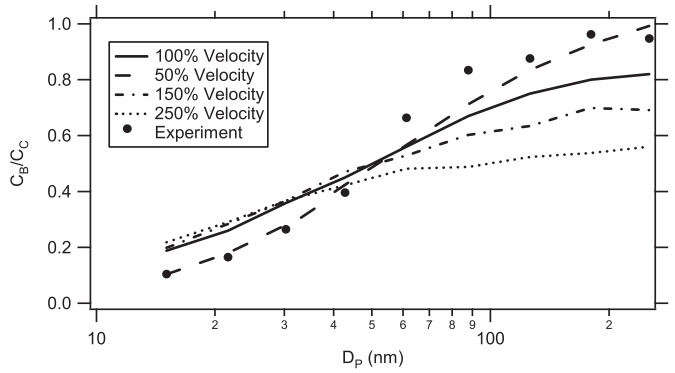

Fig. 9. Comparison of concentration ratio between the barrier and the no-barrier sites, C_B/C_C, for varying multiples of inlet velocity.

reduction of concentration. For the smaller size ranges, we see only a moderate difference in C_B/C_C for the various wind speeds. In this size range, diffusion has a much greater effect than impaction. Therefore, we expect the net effect to be an increase in C_B/C_C as velocity increases, though this effect appears to be small. Impaction becomes more important than diffusion as the particle size increases. Thus for the larger particle sizes, the net effect is a decrease in C_B/C_C as velocity increases. Overall, it appears variation in wind speed has a much greater impact on the concentration of particles larger than 50 nm than particles smaller than 50 nm.

It is also noteworthy that the 50% velocity case shows the best overall agreement with the experimental data. As we have shown in Table 1, the simulated velocity overpredicts the velocity behind the barrier. Thus, by artificially decreasing the inlet velocity, obtaining simulated velocities closer to what was observed in the experiment, we observe an improvement in the particle concentration results. It is clear then, that further improvements must be made to the flow model in order to more accurately predict particle concentrations.

7. Conclusion and recommendations

We expanded the capability of the CTAG model to account for the effects of vegetation on both the wind flow and near-road particle size distributions. The model was evaluated using experimental field measurements from Chapel Hill, North Carolina. It is found that the model performs generally well, but underpredicts the reduction in concentration of particles smaller than 50 nm through a vegetation barrier.

Near-road environments are highly complex. While vegetation is just one aspect of this complexity, it offers a significant challenge in modeling these areas. There are areas in which these models can be improved. Most important, perhaps, is the need for improvements in the velocity simulation. It is likely that the inability of the model to fully capture velocity trends has significant impact on the particle size distributions. The model can potentially be improved by creating more detailed geometric models and/or by using more complicated CFD techniques such as Large Eddy Simulation (LES).

The model formulations for deposition found in literature are generally developed for regional-scale models. While this is useful for describing total deposition to forest canopies, which are generally modeled to be essentially homogenous, it may be necessary to develop newer models that take into consideration the inherent multi-dimensionality of the near-road environment. Because a large number of particles emitted by motor vehicles are smaller than 50 nm (Kittelson, 1998) and it was found that this size range is particularly sensitive to the model formulation, careful attention should be given to deposition of particles less than 50 nm in development of near-road deposition models.

The sensitivity analyses we performed show that increases in LAD will increase the amount of deposition that occurs. However, this increase is not a linear function of LAD and it affects different particle sizes differently. This suggests that in creating models, it is important to accurately represent the tree LAD, which is highly dependent on factors such as tree species and season. Likewise, changes in wind speed affect different particle sizes differently. It was observed that for the low wind speed category which we simulated, as wind speed increases, the concentration of particles less than 50 nm increases while the concentration of particles greater than 50 nm decreases.

As such, the aerodynamic considerations pertaining to vegetation must be handled very carefully. Realistic profiles of leaf area more accurate meteorological conditions and more detailed geometry are all areas which may need to be improved to accurately represent the flow field which ultimately drives advective transport of particulate.

Acknowledgments

We would like to thank Gayle Hagler and Richard Baldauf at the Environmental Protection Agency, Andrey Khlystov at Duke University for sharing the experimental data as well as valuable discussions on interpreting the data. We would like to thank Professors Tom Whitlow and Zellman Warhaft for their helpful suggestions and comments. We also would like Dr. Alexander Petroff at University of Toronto and Dr. Leiming Zhang at Environment Canada for sharing their particle deposition models.

References

ANSYS, 2009. ANSYS FLUENT 12.0 Theory Guide. ANSYS, Inc.

Baldauf, R., Thoma, E., Khlystov, A., Isakov, V., Bowker, G., Long, T., Snow, R., 2008. Impacts of noise barriers on near-road air quality. Atmospheric Environment 42, 7502–7507.

Bouvet, T., Loubet, B., Wilson, J.D., Tuzet, A., 2007. Filtering of windborne particles by a natural windbreak. Boundary-Layer Meteorology 123, 481–509.

Bowker, G.E., Baldauf, R., Isakov, V., Khlystov, A., Petersen, W., 2007. The effects of roadside structures on the transport and dispersion of ultrafine particles from highways. Atmospheric Environment 41, 8128–8139.

Buccolieri, R., Gromke, C., Di Sabatino, S., Ruck, B., 2009. Aerodynamic effects of trees on pollutant concentration in street canyons. Science of the Total Environment 407, 5247–5256.

Cahill, T., 2010. How does Vegetation Affect Pollution Removal. The Workshop on the Role of Vegetation in Mitigation Air Quality Impacts from Traffic Emissions. RTP, North Carolina, April 2010.

Cleugh, H.A., 1998. Effects of windbreaks on airflow, microclimates and crop yields. Agroforestry Systems 41, 55–84.

Cowan, I.R., 1968. Mass, heat and momentum exchange between stands of plants and their atmospheric environment. Quarterly Journal of the Royal Meteorological Society 98, 523–544.

Davidson, C.I., Miller, J.M., Pleskow, M.A., 1982. The influence of surface-structure on predicted particle dry deposition to natural grass canopies. Water Air and Soil Pollution 18, 25–43.

Endalew, A.M., Hertog, M., Gebrehiwot, M.G., Baelmans, M., Ramon, H., Nicolai, B.M., Verboven, P., 2009. Modelling airflow within model plant canopies using an integrated approach. Computers and Electronics in Agriculture 66, 9–24.

Finn, D., Clawson, K.L., Carter, R.G., Rich, J.D., Eckman, R.M., Perry, S.G., Isakov, V., Heist, D.K., 2010. Tracer studies to characterize the effects of roadside noise barriers on near-road pollutant dispersion under varying atmospheric stability conditions. Atmospheric Environment 44, 204–214.

Green, S.R., Grace, J., Hutchings, N.J., 1995. Observations of turbulent air-flow in 3 stands of widely spaced sitka spruce. Agricultural and Forest Meteorology 74, 205–225.

Green, S.R., 1992. Modelling turbulent air flow in a stand of widely-spaced trees. The PHOENICS Journal of Computational Fluid Dynamics and Its Applications 5 (3), 294–312.

Gromke, C., Buccolieri, R., Di Sabatino, S., Ruck, B., 2008. Dispersion study in a street canyon with tree planting by means of wind tunnel and numerical investigations – Evaluation of CFD data with experimental data. Atmospheric Environment 42, 8640–8650.

Gromke, C., Ruck, B., 2007. Influence of trees on the dispersion of pollutants in an urban street canyon – Experimental investigation of the flow and concentration field. Atmospheric Environment 41, 3287–3302.
Hagler, G.S.W., Lin, M., Khlystov, A., Baldauf R.W., Isakov, V., Faircloth, J., Jackson, L., in press. Roadside vegetative and structural barrier impact on near-road ultrafine particle concentrations under variable meteorological conditions. Science of the Total Environment.
HEI, 2010. Traffic-related Air Pollution: A Critical Review of the Literature On Emissions, Exposure, and Health Effects. HEI Special Report 17. Health Effects Institute, Boston MA.
Heist, D.K., Perry, S.G., Brixey, L.A., 2009. A wind tunnel study of the effect of roadway configurations on the dispersion of traffic-related pollution. Atmospheric Environment 43, 5101–5111.
Hiraoka, H., Ohashi, M., 2008. A (k-epsilon) turbulence closure model for plant canopy flows. Journal of Wind Engineering and Industrial Aerodynamics 96, 2139–2149.
Jacobson, M.Z., 2005. Fundamentals of atmospheric modeling. Fundamentals of Atmospheric Modeling.
Jones, W.P., Launder, B.E., 1972. Prediction of laminarization with a 2-equation model of turbulence. International Journal of Heat and Mass Transfer 15, 301–314.
Kaimal, J.C., Finnigan, J.J., 1994. Atmospheric Boundary Layer Flows: Their Structure and Measurement. Oxford University Press.
Kittelson, D.B., 1998. Engines and nanoparticles: a review. Journal of Aerosol Science 29, 575–588.
Lalic, B., Mihailovic, D.T., 2004. An empirical relation describing leaf-area density inside the forest for environmental modeling. Journal of Applied Meteorology 43, 641–645.
Liu, J., Chen, J.M., Black, T.A., Novak, M.D., 1996. E-ε modelling of turbulent air flow downwind of a model forest edge. Boundary Layer Meteorology 77 (1), 21–44.
Massman, W., 1987. A comparative-study of some mathematical-models of the mean wind structure and aerodynamic drag of plant canopies. Boundary-Layer Meteorology 40, 179–197.
Petroff, A., Zhang, L., Pryor, S.C., Belot, Y., 2009. An extended dry deposition model for aerosols onto broadleaf canopies. Journal of Aerosol Science 40, 218–240.
Petroff, A., Zhang, L., 2010. Development and validation of a size-resolved particle dry deposition scheme for applications in aerosol transport models. Geoscientific Model Development Discussion 3, 1317–1357.
Piskunov, V.N., 2009. Parameterization of aerosol dry deposition velocities onto smooth and rough surfaces. Journal of Aerosol Science 40, 664–679.
Raupach, M.R., Thom, A.S., 1981. Turbulence in and above plant canopies. In: Van Dyke, M., Wehausen, J.V., Lumley, J.L. (Eds.), Annual Review of Fluid Mechanics, vol. 13. Annual Reviews, Inc, Palo Alto, Calif., USA, p. X+530. Illus: P97–130.
Raupach, M.R., Woods, N., Dorr, G., Leys, J.F., Cleugh, H.A., 2001. The entrapment of particles by windbreaks. Atmospheric Environment 35, 3373–3383.
Santiago, J.L., Martin, F., Cuerva, A., Bezdenejnykh, N., Sanz-Andres, A., 2007. Experimental and numerical study of wind flow behind windbreaks. Atmospheric Environment 41, 6406–6420.
Shimeta, J., Jumars, P.A., 1991. Physical mechanisms and rates of particle capture by suspension-feeders. Oceanography and Marine Biology: An Annual Review 29, 191–257.
Slinn, W.G.N., 1982. Predictions for particle deposition to vegetative canopies. Atmospheric Environment 16, 1785–1794.
Thom, A.S., 1972. Momentum, mass and heat-exchange of vegetation. Quarterly Journal of the Royal Meteorological Society 98, 124–134.
Tong, Z., Wang, Y., Patel, M., Kinney, P., Chillrud, S., Zhang, K.M., 2012. Modeling spatial variations of black carbon particles in an urban highway-buildings environment. Environmental Science & Technology 46 (1), 312–319.
Walklate, P.J., Weiner, K.L., Parkin, C.S., 1996. Analysis of and experimental measurements made on a moving air-assisted sprayer with two-dimensional air-jets penetrating a uniform crop canopy. Journal of Agricultural Engineering Research 63, 365–377.
Wang, H., Takle, E.S., Shen, J.M., 2001. Shelterbelts and windbreaks: mathematical modeling and computer simulations of turbulent flows. Annual Review of Fluid Mechanics 33, 549–586.
Wang, Y.J., DenBleyker, A., McDonald-Buller, E., Allen, D., Zhang, K.M., 2011. Modeling the chemical evolution of nitrogen oxides near roadways. Atmospheric Environment 45, 43–52.
Wang, Y.J., Zhang, K.M., 2009. Modeling near-road air quality using a computational fluid dynamics model, CFD-VIT-RIT. Environmental Science & Technology 43, 7778–7783.
Wang, Y., Nguyen, M, Steffens, J., Tong, Z., Wang, Y-H., Hopke, P.K., Zhang, K.M., submitted for publication. Simulating transport and transformation of multi-pollutants in complex environments: Part II: Modeling particle size distributions and micro-environmental air quality near a large highway intersection. Atmospheric Environment.
Wang, Y., Zhang, K.M., submitted for publication. Simulating transport and transformation of multi-pollutants in complex environments: Part I: Development of the Comprehensive Turbulent Aerosol Dynamics and Gas Chemistry (CTAG) Model. Atmospheric Environment.
Wilson, J.D., 2004a. Oblique, stratified winds about a shelter fence. Part I: measurements. Journal of Applied Meteorology 43, 1149–1167.
Wilson, J.D., 2004b. Oblique, stratified winds about a shelter fence. part II: comparison of measurements with numerical models. Journal of Applied Meteorology 43, 1392–1409.
Wilson, N.R., Shaw, R.H., 1977. Higher-order closure model for canopy flow. Journal of Applied Meteorology 16, 1197–1205.
Yamartino, R.J., 1984. A comparison of several single-pass Estimators of the standard-deviation of wind direction. Journal of Climate and Applied Meteorology 23, 1362–1366.
Zhang, K.M., Wexler, A.S., 2004. Evolution of particle number distribution near roadways – Part I: analysis of aerosol dynamics and its implications for engine emission measurement. Atmospheric Environment 38, 6643–6653.
Zhang, K.M., Wexler, A.S., Zhu, Y.F., Hinds, W.C., Sioutas, C., 2004. Evolution of particle number distribution near roadways. Part II: the 'road-to-ambient' process. Atmospheric Environment 38, 6655–6665.
Zhang, L., Wright, L.P., Blanchard, P., 2009. A review of current knowledge concerning dry deposition of atmospheric mercury. Atmospheric Environment 43, 5853–5864.
Zhang, L.M., Gong, S.L., Padro, J., Barrie, L., 2001. A size-segregated particle dry deposition scheme for an atmospheric aerosol module. Atmospheric Environment 35, 549–560.